Preliminary Investigation of WSR-88D Data for Winter Hydrometeorological Events in Upstate New York

R.E. HOUCK[1], J.S. WALDSTREICHER[2], J.M. HASSETT[1] AND P.F. BLOTTMAN[2]

ABSTRACT

For five case storms from January to March, 1995, radar reflectivity data obtained from the Binghamton, New York WSR-88D ground radar were compared to ground measurements acquired using a snowboard network located at the Heiberg Research Forest in Tully, New York. The WSR-88D was evaluated for its potential in measuring snowfall rate and snow water equivalent for three of the distinct types of snowstorms that affect central New York: Great Lakes lake-effect, overrunning (Gulf-origin) and Atlantic coastal storms. Level IV base reflectivity values were recorded from each volume scan for the one pixel (1 km x 1 km) above the Heiberg Forest site and for a larger 9 pixel block encompassing the Forest (3 km x 3 km).

A regression of reflectivity (Z) on snow water equivalent precipitation rate (W) produced higher correlations for the Atlantic and overrunning storms (R^2 = 0.24 and 0.35) than for the two lake effect storms studied (R^2 = 0.13 and 0.16). All snowstorms showed a much stronger reflectivity correlation with the snow accumulation rate (S). For these Z-S regressions, the Atlantic and overrunning storms produced R^2 values of 0.73 and 0.57 respectively and the lake effect storms had R^2 values of 0.15 and 0.31. Use of the 9 pixel average reflectivity values did not improve the Z-W nor the Z-S correlations. A regression of reflectivity on W and S for all storms events combined produced an R^2 value of 0.28 for Z-W and 0.17 for Z-S for the one pixel values. Removing storm 1 (very high reflectivity due to sleet and rain) from the combined storm regression, improved the R^2 values to 0.29 for Z-W and to 0.34 for Z-S.

Key words: snowfall measurement; radar; WSR-88D; snowstorm characteristics

INTRODUCTION

Snow accounts for up to 40% of the annual precipitation total in central, northern and western New York watersheds. Snowfall is, in general, highly variable in time and space, particularly in lake effect snow belt regions. Accurate snow accumulation and snow water equivalent data are needed for short term (0-3 day) flooding forecast and hydropower scheduling decisions, intermediate term (3-5 day) river level and streamflow forecasts and longer term (seasonal) water resource management decisions. Real-time measurement of snow precipitation will also allow earlier warning of severe winter storm events.

The National Weather Service WSR-88D ground-based radar network is an available source of quantitative, spatially distributed precipitation measurements that can provide a real-time and cost-effective means of estimating snowfall rate and snow water equivalent (SWE) over an extensive area. While early results from the WSR-88D are very promising in terms of accurately measuring rainfall intensity and rainstorm totals (Amburn and Fortin, 1993), the utility of the WSR-88D for accurately measuring snowfall intensity and accumulation has not yet been established.

In a Cooperative Program for Operational Meteorology, Education and Training (COMET) Partners Project between the SUNY College of Environmental Science and Forestry (SUNY-ESF) in Syracuse, NY and the National Weather Service Office (NWSO) in Binghamton, NY, the performance of the Binghamton WSR-88D ground radar was examined for estimating localized snowfall during the winter of 1995. The main objectives of the study were to (1) establish the reflectivity and meteorological characteristics of the various central NY snowstorms; (2) assess the capabilities of the WSR-88D radar for estimating snowfall rate and SWE rate for these storms by correlating radar and ground measurements; and (3) identify further research areas for utilizing the WSR-88D radar for snowfall measurement. This study

[1] State University of New York College of Environmental Science and Forestry, Division of Environmental and Resource Engineering, 312 Bray Hall, One Forestry Drive, Syracuse, New York 13210-2778

[2] National Weather Service Office, Binghamton Regional Airport, 32 Dawes Drive, Johnson City, New York 13790

was designed to guide future efforts at establishing usable Z-W and Z-S relationships for the WSR-88D for different snowstorm types. An explicit determination of the Z-W or Z-S algorithm was not sought from the data comparisons.

Snowfall and SWE data estimated from the WSR-88D could eventually be integrated with data from precipitation gauges and from remote sensing (e.g., the airborne snow survey program) to produce a reliable yearly snow database over an extensive area to be used for longer term water resource management decisions. The NWS River Forecast Centers (RFCs) routinely utilize such storm and seasonal snowpack SWE data to assess flooding potential for rivers and streams.

BACKGROUND

Ground, airborne and satellite snowfall measurement

Measurements of snowfall and SWE are currently gathered at either specific ground locations (weather service offices, cooperative observers, snow courses, SNOTEL networks) or remotely sensed from low-flying aircraft using terrestrial gamma radiation detection systems. The sparse (in terms of density) network of snow gauges, snow courses and observers provides a limited means to estimate storm snowfall total just as a sparse network of rain gauges provides a limited means to estimate rainfall totals (Lebel, *et al.*, 1987 and Peters-Lidard and Wood, 1994). Although the airborne gamma radiation snow survey program has been established as a reliable estimator of snow water equivalent (Carroll, *et al.*, 1988), coverage by a single aircraft is limited and infrequent. Individual flightlines are typically 16 km long by 300 meters wide, covering 5 km^2. The NWS Office of Hydrology operates only two such aircraft nationally, usually limiting overflights of a specific area to two to four times per year (NOHRSC, 1992).

Areal snow coverage (but not SWE) is acquired from the Advanced Very High Resolution Radiometer (AVHRR) on the NOAA polar orbiting satellites (NOHRSC, 1992). Current research is investigating the use of shortwave infrared sensors aboard the Landsat Thematic Mapper to measure snowcover extent at 1 km x 1 km resolution (Hall, *et al.*, 1995). The satellite-borne Special Sensor Microwave Imager (SSMI) is also being evaluated as a passive microwave technology for measuring snow water equivalent. With this method, microwave brightness temperatures are used to determine SWE. However, the maximum resolution is 150 km^2 (Woo, *et al.*, 1995).

Radar measurement of snowfall

Ground-based radar measurement of snowfall offers distinct advantages over the previously described snow cover and SWE estimation methods. This technology can provide real-time measurement of snow events at resolutions below 1 km^2. The 166,000 km^2 areal coverage of this radar site encompasses central New York, northeastern Pennsylvania and northern New Jersey. Coverage is virtually continuous in time, and more easily obtained than satellite or airborne data or imagery.

Studies during the last four decades have attempted to establish a usable relationship between radar reflectivity (Z) and SWE rate (W), snowfall accumulation rate (S) or rainfall rate (R) for use in real-time forecasting and determining storm and seasonal precipitation totals. An algorithm of the form $Z=aW^b$ is most often used, with radar reflectivity Z described in mm^6/m^3 and W in mm/hr of liquid water. In an extensive study, Gunn and Marshall (1958) produced the most widely referenced Z-W relationship. Analyzing snow diameter distributions of falling snow, they found the sum of the sixth powers of the melted snow particle diameters (a measure of reflectivity) to be related to the precipitation rate by $Z=2000W^{2.0}$. Sekhon and Srivastava (1970) reanalyzed and combined existing Z-W studies and snow particle size distributions to produce a similar Z-W relationship of $Z=1780W^{2.21}$. They also arrived at a water equivalent to snowfall rate relationship of $W=0.250S^{0.86}$ and a particle diameter to snowfall rate relationship of $D=0.14S^{0.45}$. Carlson and Marshall (1972) utilized 140 snow observing stations within 160 km of a CPS-9 3.2 cm radar to track a 36 hour storm over Montreal, Canada. The researchers found that 68% of the radar-estimated snow values within 70 kilometers of the radar were within 0.76 to 1.32 times the ground recorded snow depth. Boucher and Wieler (1984) also used a CPS-9 3.2 cm radar to study six Massachusetts snowstorms during 1978. Radar reflectivity values were correlated to snowfall accumulation measured with snowboards at seven sites within a 50 km range. The researchers established one relationship of $Z=5.07S^{1.65}$ for all storms. Using this algorithm, 68% of the radar-derived values were found to be within +41% to -29% of ground reference values for hourly snowfall rates and +44% to -31% for storm total accumulation. Fujiyoshi et al. (1990) used three snow gauging stations within 9 km of a Hokkaido, Japan CPS-9 radar site to measure a rimed, dendritic snowfall event. They found $Z=427W^{1.09}$ for 1 minute integrated snowfall rates and $Z = 554W^{0.88}$ for 30 minute integrated snowfall rate totals. In earlier work, Battan (1973) summarized various studies of the

reflectivity factor/snowfall intensity relationship showing the Z-W algorithm to range from $Z=600W^{1.8}$ to $Z=1780W^{2.21}$.

These studies have not considered snowstorm type as a variable but have attempted to accommodate all snow events with a single Z-W or Z-S algorithm. Collier (1989) demonstrated in a 1982-83 study in northwest England that different rainfall Z-R radar calibrations were needed to accurately measure rainfall rate for frontal, convective and shower storms. In many regions of the United States, snow storms vary greatly from one another in their snow crystalline shape, size and water content. Consequently, radar reflectivities from these different storms are expected to demonstrate greater variance than the reflectivity from rainstorms. Empirical research has shown that if snow particles are of uniform size for an individual storm and Rayleigh scattering is dominant (snow particle size small with respect to radar wavelength), the radar reflectivity factor is a function of the sixth power of the reflecting particle diameter ($Z \sim D^6$). For non-uniform particle distributions and Mie scattering (particle size comparable to wavelength), the power returned to the radar is a function of the effective reflectivity factor ($P_r \sim Z_e$)(Smith, 1984; Battan, 1973). Water content has also been found to be related to snow particle diameter to the third power ($W \sim D^3$) and the reflectivity factor proportional to the square of the water content ($Z \sim W^2$) (Battan, 1973).

SITES AND METHODS

Binghamton WSR-88D ground-based radar

The Binghamton WSR-88D radar installation (KBGM) at the E. A. Link Airport was well situated for the objectives of this study (Figure 1). Snowstorms of northwest, Great Lakes lake-effect, overrunning and Atlantic coastal origin reach into the area. The Oswego County and Tug Hill Plateau regions of New York, approximately 130 km north of the Binghamton radar, are areas that experience extremely heavy lake effect snow, although such snowbands are common throughout all of central New York.

The WSR-88D S-band (10.0-11.1 cm, 2700-3000 MHz) radar has an operational range of 230 km with a 1° x 1 km resolution and 460 km with a 1° x 2 km resolution (Crum and Alberty, 1993). Much of the prior research involving the WSR-88D has concentrated upon severe weather events such as tornadoes, wind shear and thunderstorms. The greater receiver sensitivity of the WSR-88D over earlier NWS radars (-8 dBZe minimum detectable signal at 50 km compared to 13 dBZe for the WSR-57) coupled with a receiver discrimination to 0.5 dBZ, strongly increase ground radar capabilities for snowfall measurement.

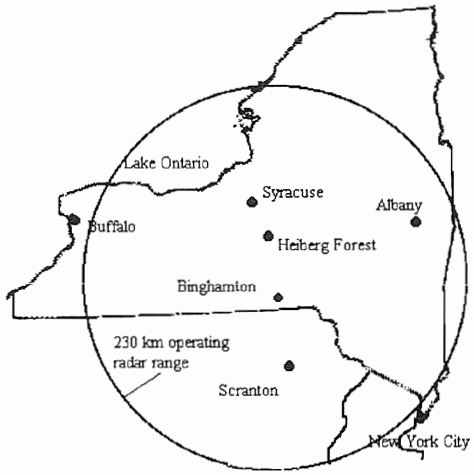

Figure 1. Location of study sites and Binghamton WSR-88D radar coverage.

The WSR-88D receiver operates in clear air mode (-28 to 28 dBZ reflectivity range) until a sufficient portion of reflectivity returns are above the 28 dBZ limit. Volume scans are completed every 10 minutes in this scanning mode. For most rainstorms and only very heavy snowfall events, the radar receiver operates in precipitation mode (5 to 75 dBZ), completing a volume scan every 5 to 6 minutes. During the 1995 winter, Level IV base reflectivity products were available from the Binghamton radar. These Level IV products are graphical depictions of the returned signal received by the radar (e.g., Level II) displayed in dBZ increments. Clear air mode Level IV base reflectivity data is displayed in 4 dBZ ranges (16 levels) and the precipitation mode is available in 5 dBZ increments (16 levels).

Heiberg Research Forest, Tully NY

The primary snow measurement site was established at the SUNY-ESF Heiberg Research Forest in Tully, NY (lat. 42° 46′ N, long. 76° 05′ W), located 55 km north of the Binghamton radar installation and 30 km south of the city of Syracuse. This 1680 hectare forest contains planted and natural growth of Norwegian spruce, red spruce, maple, cherry and beech. Snow measurement sites were located near the 610 m maximum elevation of the research forest. At this location, snowfall over the last 20 years has averaged 305 cm, with the 1992-1993 winter totaling 488 cm and 412 cm for the 1993-94 winter. Winds are predominantly from

the west and northwest, though south and southwesterly flows are not uncommon. At an elevation angle of 0.5°, the centerline of the Binghamton radar beam is at an altitude of 730 m over Heiberg Forest. Pixel size at the Heiberg Forest distance represents an area close to 1 km by 1 km.

Snowboards were constructed of 1 m x 1m, white-painted, plywood or acrylic sheets. Two snowboards were placed at each of three sites located within 700 m of one another in the Heiberg Research Forest. A Universal Weighing precipitation gauge was installed in Site 1, near the area of snowboard measurement. This site, the westernmost, has a low density compartment of young spruce 0.5 to 2 m in height. A 20 m high spruce stand lined the western edge of the compartment approximately 40 m distant from the measurement station. Spruce also lined the southern side, approximately 70 m distant. A hardwood stand was located 150 m to the north and low dense brush 20 m to the east. The snowboard measuring station in Site 2 was located adjacent to a 1.5 km^2 pond. The pond bounded the site to the east and north. Dense spruce, 8-10 m high and 20-30 m distant, lined the site to the west and south. The third snowboard measuring site was located within a medium density hardwood stand of mixed age, between the other two measurement sites.

Radar snowfall measurements

The Binghamton NWSO routinely archives base reflectivity Level IV data from the KBGM WSR-88D as per established guidelines (USDOC, 1990). For the duration of each of the five storms studied, Level IV base reflectivity dBZ values were recorded for each 10 or 6 minute volume scan (clear air or precipitation mode). This reflectivity was recorded as a dBZ range for the single pixel covering the study area within Heiberg Forest and for each of the 8 adjacent pixels in the square pixel block encompassing the Forest (3 km x 3 km). This dBZ range was converted into a Z (reflectivity) range and the midpoint of the Z range was considered to be the power of the signal received for that pixel for the given time interval. The nine pixel values were also converted to reflectivity (Z) in the same manner, but then averaged to develop one Z value for this larger area. The 6 or 10 minute, mid Z values were then averaged over time (one hour or over the duration of the ground measurement interval) to produce average hourly or average interval reflectivity values. The average Z values were converted back to dBZ values for use in some of the correlations with the ground-acquired data.

Ground snowfall measurements

At the beginning of each storm study period, the snowboards were placed on top of and level with the existing snowpack. One snowboard at each site was designated as the hourly sampling board and the other as the storm total board to be sampled at the storm's end. Snow measurements were made as close to hourly as possible during a circuit of the three snowboard stations. However, some measurement intervals reached 2 to 3 hours. Snow depth was measured using a graduated rule on the board. SWE was calculated by weighing a snow sample removed from the board in a measuring can of known diameter. A Taylor-LaChapelle Snow Density Kit scale (0-100 g range and readable to the nearest gram) was used for weighing the snow samples. The hourly sampling boards were cleared of snow after measurement and replaced at an undisturbed snowpack location within the site to prepare for the next hourly measurement. At the time of each snowboard measurement, a hand lens was used to note the size and shape of the falling snow particles. During the second through fifth storm events, the precipitation gauge was set to a 24 hour recording cycle, allowing quarter-hour SWE measurement to the nearest 0.01 inch.

The snowboard measurements were averaged over the time interval between measurements to produce hourly SWE rates (W) and hourly snow accumulation rates (S). The precipitation gauge data was also reduced to hourly SWE rates for comparison to the snowboard values. The snow depth to SWE ratio (S/W) was calculated hourly and also for the entire storm to investigate S/W differences between the types of snowstorms.

Ground and radar data linking

The fundamental work in this study consisted of comparing processed radar reflectivity data with observed snowfall data. Although the snow precipitation rate aloft and at ground level, at one location, will vary due to wind effects during snowfall, these rates were considered to be equal for an initial comparison. The larger area 9 pixel block average reflectivity values were used as a means to help reduce these discrepancies.

To assess the correlation between the radar and ground snowfall measurements, the obtained average hourly reflectivity Z and dBZ values were matched to the snowboard hourly or interval average snow accumulation and SWE rates. Using the reflectivity for one the pixel and for the 9 pixel block Heiberg cells, Z and dBZ were correlated with S and W for the five separate storms and for all the storms

combined. Reflectivity returns were also correlated to the S/W ratio for individual and combined storms.

RESULTS

Central New York experienced a mild 1994-95 winter in terms of snowfall and cold temperatures. Heiberg Research Forest recorded 118 cm of snowfall during the entire winter, far under the normal 300 cm + seasonal snowfall. Ground and radar measurements were taken for the five largest snow events during the period from January 6 to March 9, 1995. The meteorological development of each the five events is described here.

Storm Summaries

Storm 1 - Overrunning - January 6-7, 1995
A weakening surface low moved from the Ohio Valley on the evening of January 6th to New York City by the morning of January 7th. An overrunning pattern associated with weak warm air advection overspread central New York ahead of this storm, resulting in a period of light precipitation. However, low-level temperatures were marginal for frozen precipitation. Dry air in the lowest level of the atmosphere caused some evaporative cooling that did result in a period of snow at the onset of precipitation. Soon, snow changed to ice pellets, needles and finally rain.
(Snowfall total: 21 mm; SWE: 4.5 mm; S/W ratio: 5)

Storm 2 - Lake effect - January 26-27, 1995
An arctic outbreak brought a multi-band lake effect snow event to central New York on the evening of January 26th and into the 27th. The over-lake fetch of the storm was 290° at the onset, veering to 310° near the end of the event. Only minimal directional wind shear was present and temperatures between the low atmospheric levels and the lake surface brought extreme instability (17°C between lake surface and 850 mb) to the area. (Snow crystal structure: spatial dendrites with diameter 3-5 mm; Snowfall total: 36 mm; SWE:2.5 mm; S/W ratio: 16)

Storm 3 - Atlantic coastal - February 4-5, 1995
A southeast flow of Atlantic moisture ahead of a storm developing over the Carolinas overspread the region during the pre-dawn hours of February 4th and continued all day as the storm moved up the East coast. By evening the winds shifted to northwest, bringing in bitterly cold Arctic air. (Snow crystal structure: spatial dendrites 1-2 mm in diameter, plates and some stellar crystals; Snowfall total: 150 mm; SWE: 12.5 mm; S/W ratio: 12)

Storm 4 - Lake effect - February 24-25, 1995
Northwest winds with little directional wind shear resulted in multiple snowbands downwind of Lake Ontario in central New York. The snowbands eventually organized into a single intense snowband that persisted over or near Heiberg Forest during the morning and early afternoon hours of February 25th.(Snow crystal structure: stellar crystals 3-4 mm in diameter and spatial dendrites, some capped columns were observed; Snowfall total: 193 mm; SWE: 8.1 mm; S/W ratio: 24)

Storm 5 - Overrunning/Atlantic - March 8-9 1995
A cold front moving across central New York on the morning of March 8th stalled along the Atlantic seaboard as low pressure developed over the Carolinas and moved northeast. This advancing low pressure front transported Atlantic moisture up and over the deepening cold air dome across central New York. Rain changed to sleet and then to snow as the front moved through the region. (Snow crystal structure: spatial dendrites 1-2 mm in diameter and plates to a lesser extent; Snowfall total: 82 mm; SWE: 10.6 mm; S/W ratio: 8)

Individual Storms: Z-W and Z-S correlations

For the five events, a total of 134 snowboard measurements were taken of snow depth and SWE. The hourly average reflectivity (Z) was regressed on the SWE hourly rates (W) for the individual storms 1-5. A power function of the form $y= ax^b$, similar to the $Z=aW^b$ algorithms of previous research, was used to describe the correlation between the data sets. Figures 2a-e show the Z-W relationship for the individual storms using the one Heiberg pixel reflectivity values. Storm 1 demonstrated a negative association between the data sets while the other 4 storms resulted in fairly low positive correlations (R^2 from 0.13 to 0.35). Regressing the 9 pixel average hourly reflectivity values upon W (Figures 3a-e) did not improve the Z-W association for any of the five snow events. The lake effect storms (storms 2 and 4) showed the weakest Z-W correlation, while the overrunning and Atlantic coastal storms (storms 3 and 5) had stronger Z-W correlation.

The one pixel and the 9 pixel reflectivity values (Z) were then regressed on the hourly accumulation rate (S) for the five snow events (Figures 4a-e and 5a-e). For the one pixel, the strength of the association increased greatly over the Z-W regressions, with R^2 improvements ranging from

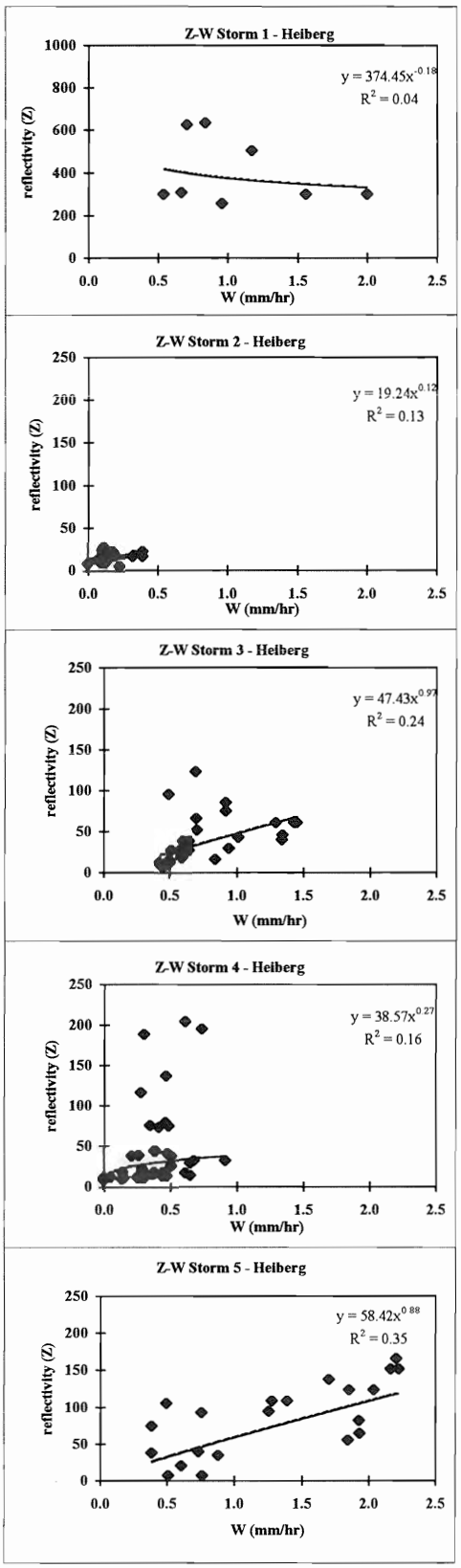

(a) Overrunning snowstorm.

(b) Lake-effect snowstorm.

(c) Atlantic coastal snowstorm.

(d) Lake-effect snowstorm.

(e) Overrunning/ Atlantic coastal snowstorm.

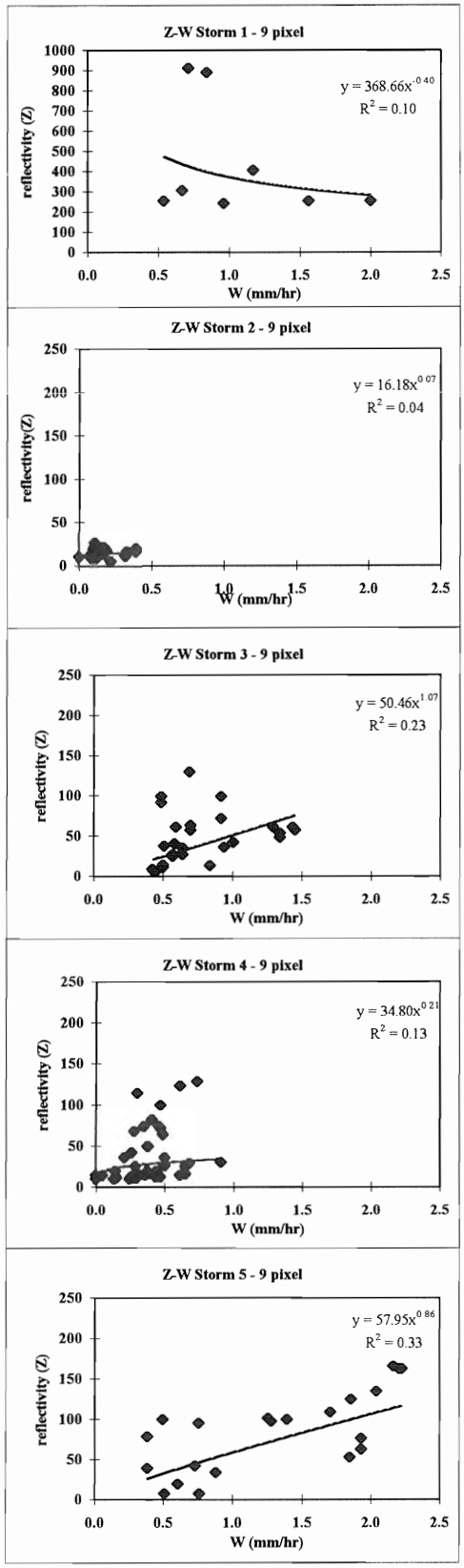

Figures 2a-e. Reflectivity (Z) correlation with snow water equivalent rate (W) by storm. One pixel values.

Figures 3a-e. Reflectivity (Z) correlation with snow water equivalent rate (W) by storm. 9 pixel values.

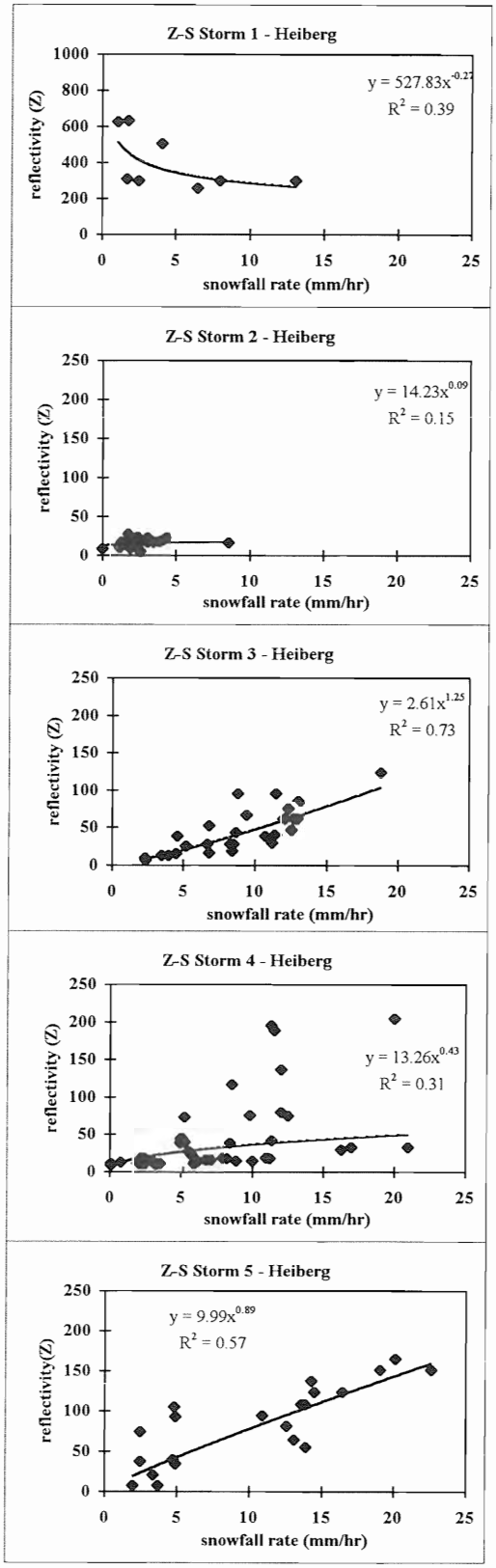

(a) Overrunning snowstorm.

(b) Lake effect snowstorm.

(C) Atlantic coastal snowstorm.

(d) Lake effect snowstorm.

(e) Overrunning/ Atlantic coastal snowstorm.

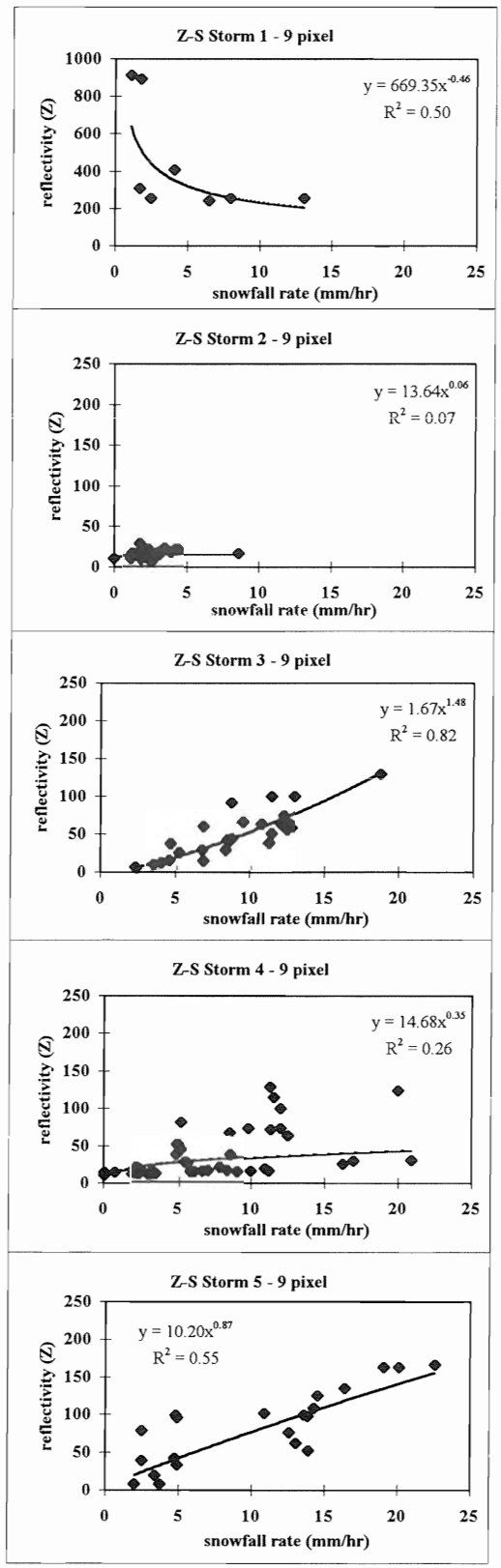

Figures 4a-e. Reflectivity (Z) correlation with snow accumulation rate (S). One pixel.

Figures 5a-e. Reflectivity (Z) correlation with snow accumulation rate (S). 9 pixel.

0.02 to 0.49 and an average R^2 improvement of 0.25. The Z-S 9 pixel correlations showed similar improvements over the Z-W 9 pixel correlations, but did not improve the correlation over the Z-S one pixel data. As with the Z-W regressions, the Atlantic and overrunning storms (storms 3 and 5) had stronger one pixel Z-S correlations, with R^2 of 0.73 and 0.57, than the lake effect storms (storms 2 and 4) with R^2 values of 0.15 and 0.31.

Combined storm correlations: Z-W and Z-S

The individual storm data sets were combined to produce a reflectivity regression for all storms on the SWE rate (W) and the snowfall accumulation rate (S). Figure 6a shows the low resulting R^2 value of 0.28 for the one pixel regression of Z on W. The 9 pixel reflectivity values (Figure 6b) did not improve the regression on W ($R^2 = 0.26$). Although the associations between reflectivity and snowfall rate (S) proved to be much stronger than for reflectivity and SWE rate (Z-W) for the individual storms, Figures 7a-b show that the Z-S association became weaker than Z-W for the combined storms for both the one and 9 pixel reflectivity data sets (R^2= 0.17 and 0.15).

Combined storm correlations: storms 2-5 only

Storm 1 produced the highest reflectivity of any of the five storms, but also produced the weakest association between reflectivity and SWE rate (W) or snowfall accumulation rate (S). A mix of snow, sleet and rain produced high reflectivities, even at low snowfall and SWE rates. High winds were persistent throughout the duration of storm 1, often preventing snow accumulation on the snowboards. During storm 1, two snowboards were located at a site which proved to be too exposed under windy conditions for reliable snowfall measurement and were later relocated to site 3 for storms 2-5. The ground measurement data acquired from this storm was therefore not considered to be accurate of the precipitated snowfall. Regression of reflectivity on SWE (W) for combined storms 2 to 5 (Figures 8a-b) did not improve the correlation over the combined storm 1-5 regression. However, for the combined storm 2-5 reflectivity regression on S, Figures 9a-b do show a doubling of the R^2 value (0.17 to 0.34) over the combined storm 1-5 Z-S regression. Here again, the 9 pixel reflectivity regressions did not improve the correlation on W or S over the one pixel regressions.

Reflectivity to S/W ratio

Reflectivity was regressed on the snow accumulation rate to SWE (S/W) ratio for the five individual storms (Figures 10a-e). The overrunning and Atlantic storms exhibited better reflectivity associations with the S/W ratio than the lake effect events. The overrunning storm 5 showed a quite high R^2 of 0.77 and also had the narrowest S/W range of the five storms. The lake effect storms exhibited a very wide range of depth/SWE ratios ranging from 5 to almost 40 and also displayed the lowest S/W correlations with reflectivity.

DISCUSSION

Storm reflectivity characteristics

The snowfall totals, crystal characteristics and correlation strengths for each of the three types of storms studied are summarized in Table 1. Although most storms did not present a high Z-W correlation in this limited study, several relationships and storm characteristics were apparent. For all storms, snow accumulation rate (S) correlated much better with reflectivity than did the SWE rate (W). These results indicate that snow particle size might have a greater influence on radar reflectivity than does water content. The heavier Atlantic and overrunning storms produced better correlations to reflectivity than did the lake effect storms. Further, the lake effect storms produced the highest S/W ratios, due mostly to the large size of the associated stellar crystals. However, these large crystals generally produced low reflectivity and had lower water content.

The individual storms did not display similar Z-W relationships. The combined storm Z-W correlations did not significantly improve the Z-W correlation over the individual storms. For the Z-S regressions, the combined storm correlations were far weaker than those of the individual storms, two of which had quite high correlations. This supports the hypothesis that the different snowstorm types will produce significantly distinct reflectivity returns and cannot be adequately described by a single Z-W or Z-S algorithm.

Causes of variation

The often low Z-W correlations could have been caused in part by several factors. First, the small number and magnitude of the snow events studied restricted the ability to make strong inferences from the study. Second, wind drift of precipitating snow produced an uncertainty as to whether atmospheric (e.g., radar) and ground measurements were of the

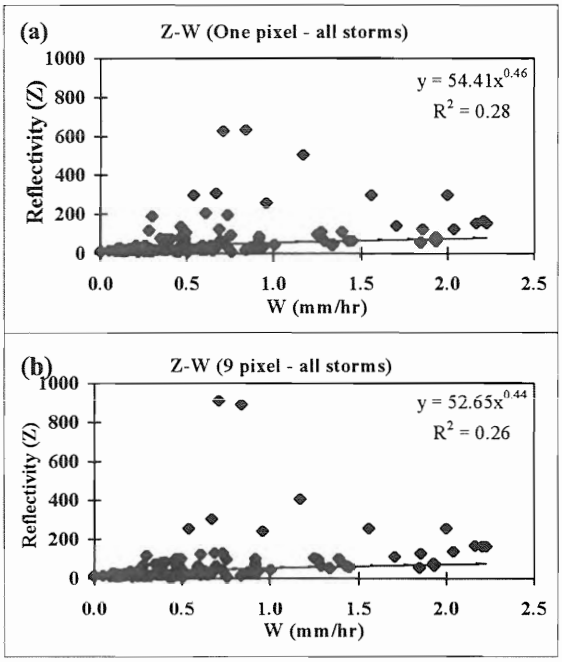

Figures 6a-b. Reflectivity correlation to SWE rate (W) for combined storms.

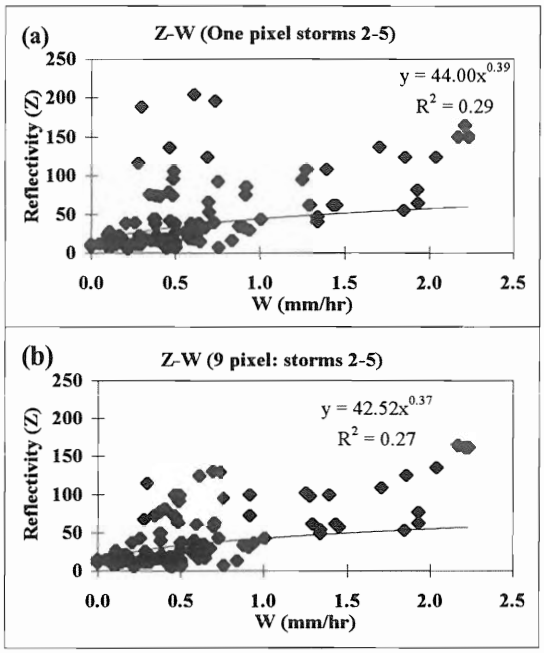

Figures 8a-b. Reflectivity correlation to SWE rate (W) for combined storms 2-5.

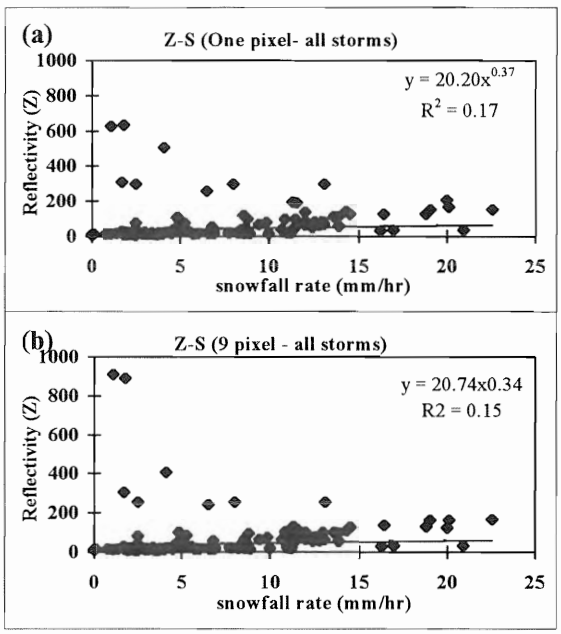

Figures 7a-b. Reflectivity correlation to snow accumulation rate (S) for combined storms.

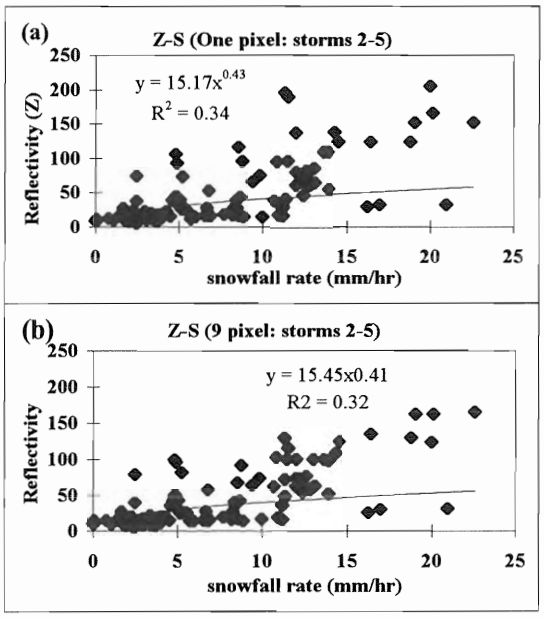

Figures 9a-b. Reflectivity correlation to snow accumulation rate (S) for combined storms 2-5.

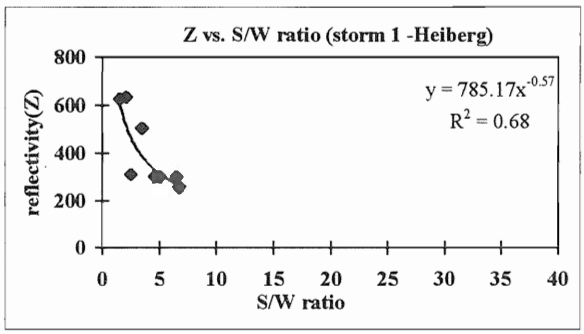

(a) Storm 1: Overrunning

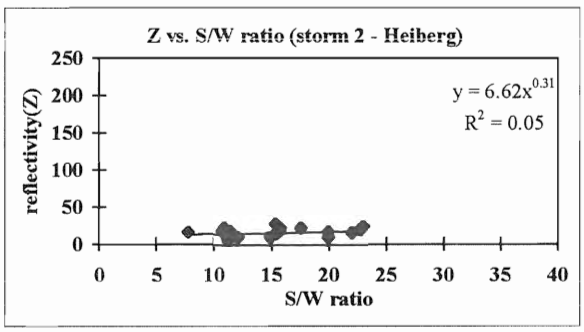

(b) Storm 2: Lake effect

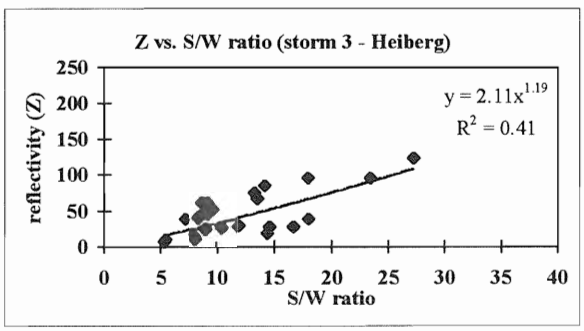

(c) Storm 3: Atlantic coastal

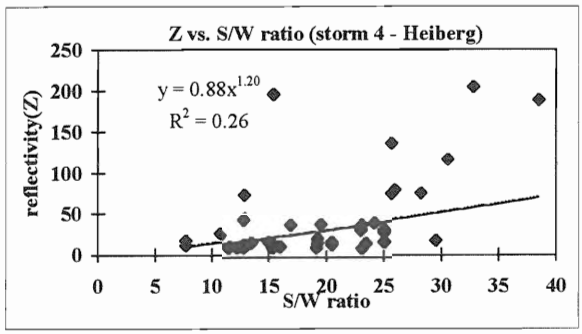

(d) Storm 4: Lake effect

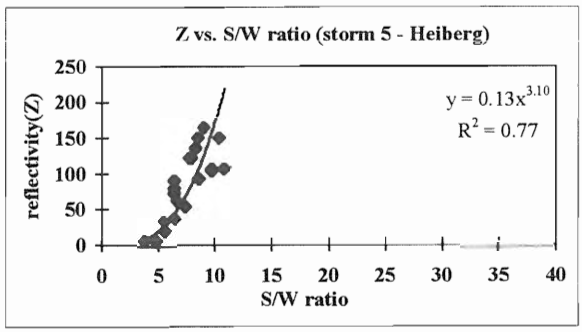

(e) Storm 5: Overrunning/Atlantic coastal

Figures 10a-e. Correlation of storm reflectivity with the snow depth/SWE ratio (S/W).

Table 1. Snow crystal and reflectivity characteristics by storm type.

Storm type	Snow crystal type and size	S/W ratio	Reflectivity characteristics
Atlantic	spatial dendrites 1-2 mm in diameter; plates	5-26	• fair to poor Z-W correlation • highest Z-S correlation of $R^2 = 0.73$ • moderately varying S/W ratio of 3 storm types
lake effect	stellar crystals 3-5 mm in diameter; spatial dendrites and some capped columns	5-38	• lowest Z-W and Z-S correlations of storm types • lowest SWE rates recorded (0-1.0 mm/hr) • highest snow depth/SWE ratios • generally low reflectivity returned
overrunning	needles, assemblages of dendrites 1-2 mm in diameter; some plates	4-10	• highest Z-W correlation (storm 5 $R^2 = 0.35$) • heaviest SWE rates up to 2.5 mm/hr and snowfall rates to 25 mm/hr • good Z-S correlation (R^2 of 0.57) • narrowest S/W ratio of three storm types and highest Z-S/W correlation

same precipitation. Use of the nine pixel average reflectivity values did not improve the Z-W or Z-S correlations over the one Heiberg pixel correlations. A third factor was the use of the Level IV dBZ range values for reflectivity measurement. Use of mid dBZ value of this 4 or 5 dBZ reflectivity display range as the actual reflectivity can introduce up to a 2.5 dBZ error. Lastly, the snow measurement scale used for the snowboard SWE measurements was not of high sensitivity. Readings were made to the nearest gram, possibly introducing significant error for the lighter measurements. Forty-nine percent of the scale measurements fell into the 4 to 15 g range, 37% from 0 to 3 g and 14% over 15 g.

Continuing Research

Further efforts will incorporate data from the NWS Nested Grid Model (Hoke, *et al.*, 1989) to examine whether atmospheric variables can help explain some of the variability of the radar reflectivity and snowfall characteristics as a function of storm type. Temperature and moisture parameters from hourly model forecast soundings above Syracuse, New York (30 km north of the study site), will be integrated into the data set. These data will be evaluated to see if correlations exist between the atmospheric variables and the reflectivity to snowfall and SWE relationships. Finally, thanks to the recent recorder installations around the country, including Binghamton, future efforts will be able to incorporate archived Level II WSR-88D base data. This will allow the use of reflectivity values to the nearest 0.5 dBZ, strengthening the radar measurement aspects of these studies.

CONCLUSIONS

Clearly, there is much work to be done before WSR-88D radar reflectivity data can be transformed to snowfall accumulation and SWE rates for use in routine forecasts and water resources decisions. The work herein represents a first step in that radar reflectivity data was compared to "ground truth" at one station. This work identified opportunities for more quantitative follow-up studies that might include steps toward development of WSR-88D Z-W and Z-S algorithms.

ACKNOWLEDGMENTS

The authors wish to thank Steve Kuhl, Scientific Services Division, NWS Eastern Region, for his comments and suggestions. The authors also thank the staff of the Heiberg Research Forest for their help in the field portion of the study.

This COMET Partners Project was funded from a subaward under a cooperative agreement with the National Oceanic and Atmospheric Administration (NOAA) and the University Corporation for Atmospheric Research (UCAR).

REFERENCES

Amburn, S.A. and S. Fortin, 1993. Use of WSR-88D and surface rain gauge network data in issuing flash flood warnings and main stem flood forecasts over Osage County, Oklahoma, June 5, 1991. USDOC NOAA Technical Memorandum, NWS ER-87, 3rd National Heavy Precipitation Workshop, Eastern Region, April 1993, 321-330.

Battan, L. S., 1973. Radar Observation of the Atmosphere. University of Chicago Press, Chicago, IL., 1973.

Boucher, R.J. and J.G. Wieler, 1984. Radar determination of snowfall rate and accumulation. *Journal of Climate and Applied Meteorology,* vol. 24, 68-73.

Carlson, P.E. and J.S. Marshall, 1972. Measurement of snowfall by radar. *Journal of Applied Meteorology,* vol. II, 494-500.

Carroll, T.R., E.L. Peck and D.M. Lipinski, 1988. Proceedings of the Annual Convention. American Congress on Surveying and Mapping and the American Society for Photogrammetry and Remote Sensing, St. Louis, MO, March 13-18, 1988.

Collier, C.G., 1989. Applications of weather radar systems. Ellis Horwood Limited, Chichester, England, 1989.

Crum, T.D. and R.L. Alberty, 1993. The WSR-88D and the WSR-88D Operational Support Facility. Bulletin of the American Meteorological Society, vol. 74, no. 9, September, 1993, 1669-1687.

Fujiyoshi, Y., T. Endoh, T. Yamada, K. Ksuboki, Y. Tachibana and G.Wakahmna, 1990. Determination of a Z-R relationship for snowfall using a radar and high sensitivity snowgauges. *Journal of Applied Meteorology,* vol. 29, 147-152.

Gunn K.L.S. and J.S. Marshall, 1958. The distribution with size of aggregate snowflakes. *Journal of Meteorology,* **15,** 452-466.

Hall, D.K., J.L. Foster, A.T.C. Chang, K.S. Brown and G.A. Riggs, 1995. Mapping snow cover during the BOREAS winter experiment. Oral presentation given by D.K. Hall at the 52nd Annual Eastern Snow Conference, June 7-8, 1995, Toronto, Ontario, Canada.

Hoke, J.E., N.A. Phillips, G.J. DiMego, J.J Tuccillo and J.G. Sela, 1989. The regional analysis and forecast system of the National Meteorological Center. *Weather Forecasting*, **4**, 323-334.

Lebel, T. , G. Bastin, C. Obled and J. D. Cretin, 1987. On the accuracy of areal rainfall estimation: a case study. *Water Resources Research* **23**(11), 2123-2134, 1987.

National Operational Hydrologic Remote Sensing Center (NOHRSC), 1992. Airborne gamma radiation snow survey program and satellite hydrologic program, User's Guide 4.0. U.S. Department of Commerce, National Weather Service, Office of Hydrology, Minneapolis, Minnesota.

Peters-Lidard, C.D. and E.F. Wood, 1994. Estimating storm areal average rainfall intensity in field experiments. *Water Resources Research*, Vol. 30, No. 7, 2119-2131, July, 1994.

Sekhon, R. S. and R.C. Srivastava, 1970. Snow size spectra and radar reflectivity. *Journal of the Atmospheric Sciences,* vol. 27, March 1970, 299-307.

Smith, P. L., 1984, Equivalent radar reflectivity factors for snow and ice particles. *Journal of Climate and Applied Meteorology,* vol. 23, 1258-1260.

U.S. Department of Commerce (USDOC), 1990. Doppler radar meteorological observations. Part A: system concepts, responsibilities, and procedures. Federal Meteorological Handbook No. 11, NOAA/OFCM, Washington, DC, 56 pp.

Woo, M., A. Walker, D. Yang and B.E. Goodison, 1995. Pixel scale ground snow survey for passive microwave study of the arctic snow cover. Oral presentation given by A. Walker at the 52nd Annual Eastern Snow Conference, June 7-8, 1995, Toronto, Ontario, Canada.